OPEN ACCESS Freely available online

PLOS ONE

Identification of Genes Differentially Expressed in *Myogenin* Knock-Down Bovine Muscle Satellite Cells during Differentiation through RNA Sequencing Analysis

Eun Ju Lee[1,2☯], Adeel Malik[1☯], Smritee Pokharel[1], Sarafraz Ahmad[1], Bilal Ahmad Mir[1], Kyung Hyun Cho[1], Jihoe Kim[1], Joon Chan Kong[3], Dong-Mok Lee[3], Ki Yong Chung[4], Sang Hoon Kim[5], Inho Choi[1,2]*

1 School of Biotechnology, Yeungnam University, Gyeongsan, Republic of Korea, **2** Bovine Genome Resources Bank, Yeungnam University, Gyeongsan, Republic of Korea, **3** Biomedical Manufacturing Technology Center, Korea Institute of Industrial Technology, Yeongcheon-si, Republic of Korea, **4** Hanwoo Experiment Station, National Institute of Animal Science, RDA, Pyeongchang, Republic of Korea, **5** Department of Biology, Kyung Hee University, Seoul, Republic of Korea

Abstract

Background: The expression of myogenic regulatory factors (MRFs) consisting of *MyoD*, *Myf5*, *myogenin* (*MyoG*) and *MRF4* characterizes various phases of skeletal muscle development including myoblast proliferation, cell-cycle exit, cell fusion and the maturation of myotubes to form myofibers. Although it is well known that the function of *MyoG* cannot be compensated for other MRFs, the molecular mechanism by which *MyoG* controls muscle cell differentiation is still unclear. Therefore, in this study, RNA-Seq technology was applied to profile changes in gene expression in response to *MyoG* knock-down ($MyoG_{kd}$) in primary bovine muscle satellite cells (MSCs).

Results: About 61–64% of the reads of over 42 million total reads were mapped to more than 13,000 genes in the reference bovine genome. RNA-Seq analysis identified 8,469 unique genes that were differentially expressed in $MyoG_{kd}$. Among these genes, 230 were up-regulated and 224 were down-regulated by at least four-fold. DAVID Functional Annotation Cluster (FAC) and pathway analysis of all up- and down-regulated genes identified overrepresentation for cell cycle and division, DNA replication, mitosis, organelle lumen, nucleoplasm and cytosol, phosphate metabolic process, phosphoprotein phosphatase activity, cytoskeleton and cell morphogenesis, signifying the functional implication of these processes and pathways during skeletal muscle development. The RNA-Seq data was validated by real time RT-PCR analysis for eight out of ten genes as well as five marker genes investigated.

Conclusions: This study is the first RNA-Seq based gene expression analysis of $MyoG_{kd}$ undertaken in primary bovine MSCs. Computational analysis of the differentially expressed genes has identified the significance of genes such as *SAP30-like* (*SAP30L*), *Protein lyl-1* (*LYL1*), various matrix metalloproteinases, and several glycogenes in myogenesis. The results of the present study widen our knowledge of the molecular basis of skeletal muscle development and reveal the vital regulatory role of *MyoG* in retaining muscle cell differentiation.

Citation: Lee EJ, Malik A, Pokharel S, Ahmad S, Mir BA, et al. (2014) Identification of Genes Differentially Expressed in *Myogenin* Knock-Down Bovine Muscle Satellite Cells during Differentiation through RNA Sequencing Analysis. PLoS ONE 9(3): e92447. doi:10.1371/journal.pone.0092447

Editor: Rossella Rota, Ospedale Pediatrico Bambino Gesù, Italy

Received October 28, 2013; **Accepted** February 21, 2014; **Published** March 19, 2014

Funding: This work was supported by a grant from the BioGreen 21 Program (Project no. PJ907099), Rural Development Administration, Republic of Korea. The funders had no role in study design, data collection and analysis, decision to publish, or preparation of the manuscript.

Competing Interests: The authors have declared that no competing interests exist.

* E-mail: inhochoi@ynu.ac.kr

☯ These authors contributed equally to this work.

Introduction

Skeletal muscle formation is a multi-step process that requires proliferation of myocytes, expression of muscle-specific myogenic regulatory factors (MRFs) including *MyoD*, *Myf5*, *myogenin* (*MyoG*) and *MRF4* (or *Myf6*), cell cycle withdrawal, myotube formation by the fusion of mononucleated cells and maturation of myotubes into myofibers [1], [2], [3], [4], [5]. MRFs are basic helix-loop-helix (bHLH) transcription factors [6] that cooperate with several transcription factors of the *myocytes enhancer factor-2* (*MEF2*) family [7] to regulate myogenesis. bHLH proteins also heterodimerize with E-proteins [8], enabling binding to the E-Box consensus sequence (CANNTG) present in the regulatory regions of muscle specific genes [9], [10]. Among these MRFs, *MyoD* is highly expressed during the mid-G1 phase and between the S and M phases of the cell cycle, but absent during the G0 phase [11], whereas *Myf5* is highly expressed during the G0 phase and decreases during the G1 phase [12]. *MyoG* and *MRF4* (*Myf6*) are expressed upon differentiation of myoblasts into multinucleated myotubes [13], [14], [15].

MyoG is crucial during differentiation [11], as many studies have revealed that mice lacking *MyoG* continue to identify the muscle lineage through the formation of myoblasts [16], but show high perinatal mortality due to severe skeletal muscle deficiency caused by disruption of myoblast differentiation and muscle fiber formation [17], [18]. Additionally, *MyoG*/*MyoD* and *MyoG*/*Myf5*

double knockout mice studies have shown that these mice specify the muscle lineage, but the formation of muscle fibers is disrupted, which is similar to *MyoG* knockout mice [19]. Furthermore, *MyoD* and *Myf5* are unable to compensate for the role of *MyoG* in differentiation [20], and mice that lack *MyoG* exhibit normal expression levels of *MyoD* and *Myf5* [17]. This is because *MyoG* acts downstream of *MyoD* and *Myf5* [16] in skeletal muscle differentiation. Knockout mice studies have also shown a relationship between different MRFs in which the absence of one will be compensated for by another [21], [22]. The only exception to this compensation effect of MRFs is *MyoG*, which plays a unique and non-redundant role during embryogenesis [19], whereas conditional knock-out resulted in reduced muscle mass in adults [23].

In this study, we conducted a comprehensive transcriptome analysis of primary bovine cells using $MyoG_{kd}$ and compared the expression profiles with those of the wild type using an RNA-Seq technique. We also showed that $MyoG_{kd}$ led to upregulation of genes involved in processes such as cell proliferation and DNA replication, whereas the genes involved in phosphate metabolic processes were down-regulated. Finally, potential involvement of various new genes in myogenesis was identified.

Materials and Methods

Bovine MSCs culture

Bovine muscle was collected from the hind leg skeletal muscle of 24–26 month old cattle with a body weight of 550–600 kg. The animals were handled according to a protocol approved by the Animal Care and Concern Committee of the National Institute of Animal Science, Korea. Briefly, the collected muscle was minced into fine pieces, and digested with trypsin-EDTA (GIBCO, CA, USA), and were centrifuged at 90×g for 3 min and the upper phase was passed through a 40-μm cell strainer. The filtrate was centrifuged at 2,500 rpm, pellet was collected, washed twice and cultured in Dulbecco's modified Eagle's medium (DMEM; HyClone Laboratories, UT, USA) supplemented with 10% fetal bovine serum (FBS, HyClone Laboratories) and 1% penicillin/streptomycin at 37°C under 5% CO_2. The culture medium was changed every other day. To induce differentiation, cells were allowed to grow in DMEM without reducing serum (DMEM with 10% FBS and 1% P/S) for 10, 12, 14, 16, and 18 days. MSCs isolation and culture were conducted as previously described [24].

MyoG shRNA construction and knock-down

Bovine *MyoG* shRNA was designed using nucleotide information obtained from NCBI (AB257560.1) and cloned with pRNAT-U6.2/Lenti vector (GeneScript, NJ, USA). Constructed *MyoG* shRNA or non-specific sequences (scrambled vector, $MyoG_{wd}$) were transfected to generate viral particles in 293 FT cells. After two days of transfection, the supernatant containing viral particles was collected, transduced with lentiviral particles expressing shRNAs against bovine *MyoG* or scrambled vector in MSCs (Day 8), and selected with 50 μg/ml of G418 (CABIOCHEM, CA, USA). The selected cells were allowed to differentiate and were harvested at Day 21. The following oligonucleotide was used to generate *MyoG* shRNA: sense: 5′- GGATCCCGCGCAGACT-CAAGCCGCCGGTGTTCAAGAGACACCTTCTTGAGTCTG-CGCTTTTCCAACTCHGAG-3′.

RNA extraction, library preparation and sequencing

MSCs were allowed to grow till day 10, and were transduced with either scrambled vector or *MyoG* shRNA. Cells were then allowed to grow for another 11 days, and were harvested with Trizol reagent (Invitrogen) according to the manufacturer's protocol. Total RNA was then extracted and stored in diethylpyrocarbonate-treated H_2O at −80°C until used. The mRNA in total RNA was converted into a library of template molecules suitable for subsequent cluster generation using the reagents provided in the Illumina TruSeq RNA Sample Preparation Kit (Illumina, CA, USA) according to the manufacturer's instructions. Library construction and high-throughput sequencing were carried out using an Illumina HiSeq2000 sequencing system in which each sequencing cycle takes place in the presence of all four nucleotides, leading to higher precision than methods in which only a single nucleotide is present in the reaction mixture at one time. The cycle is repeated one base at a time, creating a string of images each indicating a single base extension at a specific cluster.

Sequence quality check

The FASTQC [http://www.bioinformatics.babraham.ac.uk/projects/fastqc/] tool embedded in the web-based platform, Galaxy [25], [26], [27], was used to calculate quality control statistics describing raw sequence data from FASTQ files generated by the Illumina second generation sequencing technology (''Solexa'') [http://www.illumina.com/technology/solexa_technology.ilmn].

Mapping of RNA-Seq reads transcript assembly

TopHat [28] was used to align RNA-Seq reads against UCSC *Bos taurus* reference genome (Btau_4.6.1/bosTau7) via Bowtie, which is a very high-throughput short read aligner [29]. Bowtie is different from other general-purpose alignment tools such as BLAST [30], and shows best performance when short reads are aligned to large genomes. Bowtie is extremely fast for short reads where several reads have at least one significantly valid alignment, the reads are of high-quality, and the number of alignments reported per read is nearly 1 [29]. These mapping results were then analyzed to identify splice junctions between exons. All default parameters were used to run TopHat except the mate inner distance, for which a value of 100 was selected in the case of paired reads. The advantage of a paired end run is that both reads contain long range positional information, allowing for highly precise alignment of reads.

The aligned reads were further analyzed by Cufflinks [31] using a multifasta file (bosTau7. fa) option that can improve the precision of transcript abundance approximation by bias detection and a correction algorithm. The relative abundance of transcripts was reported as fragments per kilobase of exon per million fragments mapped (FPKM). An additional cufflinks parameter for the initial estimation procedure was used so that the reads mapping to multiple locations in the genome were accurately weighted [31]. The nucleotide sequences obtained in this study have been submitted and will be available in NCBI Short Read Archive with accession number SRR1122446 as soon as it is released. Alternatively, the data can be obtained directly from the authors.

Functional annotation cluster and pathway analysis

DAVID [http://david.abcc.ncifcrf.gov/home.jsp] functional annotation cluster analysis was performed on the list of up-regulated and down-regulated genes with a fold change of ≥4. Only those terms that reported a *p*-value of ≤0.05 and count number ≥5 genes were selected for analysis. The Gene Ontology (GO) terms of cellular component, molecular function and biological process in DAVID were employed to categorize enriched biological themes in up- and down-regulated gene lists.

Pathway mapping was performed using the KEGG Automatic Annotation Server (KAAS) [32]. The nucleotide sequences of up- and down-regulated genes were uploaded to the KAAS web server as an input using single-directional best hit (SBH) method to assign orthologs. KAAS offers functional annotation of genes in a genome via a BLAST similarity searches against a manually curated set of ortholog groups in the KEGG GENES database. KAAS assigned a KEGG Orthology (KO) number to genes in the data sets, which were mapped to one of KEGG's reference pathways.

Real time RT-PCR validation

One microgram of RNA in a reaction mixture with a total volume of 20 µl was primed with oligo $(dT)_{20}$ primers (Bioneer, Daejeon, Korea) and then reverse transcribed at 42°C for 50 min and 72°C for 15 min. Subsequently, 2 µl of cDNA product and 10 pmoles of each gene-specific primer were used for PCR, using a 7500 real-time PCR system (Applied Biosystems, Foster City, CA, USA). A Power SYBRH Green PCR Master Mix (Applied Biosystems) was used as the fluorescence source. Primers were designed with the Primer 3 software (http://frodo.wi.mit.edu) using the sequence information listed at the National Center for Biotechnology Information. Detailed information describing the primer sequences is provided in **Table S1**.

Immunocytochemistry

Cells grown in a covered glass-bottom dish were stained with Pax7 or MyoG antibody. Briefly, cells were rinsed with PBS (phosphate buffered saline), fixed in 4% formaldehyde, permeabilized by 0.2% TritonX-100, after which the signals were enhanced using an Image-iT FX signal enhancer (Invitrogen). The cells were then incubated with mouse primary Pax7 or MyoG antibody (1:50, Santa Cruz Biotechnology, CA, USA) at 4°C in a humid environment overnight. Secondary antibody (Alexa Fluor 488 goat anti-mouse SFX kit; Molecular Probes, Eugene, OR, USA) was treated for 1 hr at room temperature followed by nuclear staining with 4′,6′-diamino-2-phenylindole (DAPI; Sigma-Aldrich, MO, USA). Pictures were taken using a fluorescent microscope equipped with a digital camera (Nikon, Tokyo, Japan).

Western blot

Western blot was performed with the total protein isolated from cells. Briefly, cells washed with ice-cold PBS were lysed in RIPA lysis buffer containing protease inhibitor cocktail (Thermo Scientific, IL, USA). The protein was quantified by Bradford method using protein assay dye solution. Fifty microgram of protein was electrophoresed in 10% SDS-polyacrylamide gel after reducing at 90°C for 3 min with β-mercaptoethanol, and the protein was transferred to a PVDF membrane. Membrane was blocked and hybridized with MyoG (1:1000) or β-actin antibody (1:2000) (Santa Cruz Biotechnology) overnight at 4°C. Membrane washed in TBST was then incubated with horseradish peroxidase conjugated secondary antibody for an hour at room temperature. Finally, the membrane was developed using SuperSignal West Pico Chemiluminescent Substrate (Thermo Scientific).

Giemsa staining

Cells were washed with PBS, fixed with PBS/methanol (v/v) for 2 min, and were incubated with 0.04% Giemsa G250 solution for 30 min. cells were rinsed with distilled water and pictures were taken using a light microscope equipped with a digital camera (Nikon).

Statistical analysis

The normalized expression means were compared using Tukey's Studentized Range (HSD) to identify significant differences in gene expression. A nominal *p*-value of less than 0.05 was considered to be statistically significant. Real time RT-PCR data were analyzed by one-way ANOVA using PROC GLM in SAS package ver. 9.0 (SAS Institute, Cary, NC, USA).

Results

MyoG gene knock-down

MSCs isolated and cultured from bovine leg muscle were stained with Pax7 to determine the purity of cells. The isolated cells showed approximately 85% Pax7 positive cells (**Figure S1**). The *in vitro* cultured bovine primary cells began to differentiate without serum deprivation. The initial myotubes became visible at Day 12, and the number of myotubes increased with time (**Figure 1A**). The expression level of *MyoG*, which is known to play a role in myogenic differentiation [33], was determined by real-time RT-PCR at different time points of primary bovine cells differentiation. *MyoG* was expressed throughout differentiation; however, there was a steep increase in its expression level at Day 12, which gradually increased until Day 18 (**Figure 1B**). Similarly, Western blot analysis revealed MyoG protein expression on Day 10 and Day 16 with higher levels occurring on Day 16 (**Figure 1C**). This expression profile of *MyoG* during differentiation is in accordance with those of previous studies [34], [35]. Moreover, the cells were authenticated to be in the state of myotube formation by inspecting the nuclear expression of MyoG protein at two different time points (Day 10 and Day 16) during cell differentiation. MyoG protein expression was observed at Day 10 and 16. Day 16 showed higher MyoG nuclear expression as compared with Day 10 proliferating cells (**Figure 1D**). To identify the genes differentially expressed as a consequence of *MyoG* knock-down, MSCs were transduced with shRNA specific for *MyoG*. RNA analysis following transduction revealed the specific decline of mRNA for shRNA induced $MyoG_{kd}$ as compared to its wild type counterpart ($MyoG_{wd}$) (**Figure 1E**). Similarly, $MyoG_{kd}$ was confirmed at the protein level by Western blot analysis (**Figure 1F**). shRNA transduction against *MyoG* prohibited the nuclear expression of MyoG protein and the development of myotubes (**Figure 1G and 1H**).

Expression of myogenic marker genes

To confirm that primary bovine cells were undergoing differentiation, we verified the expression of *myosin regulatory light chain 2* (*MYL2*) and *myosin heavy chain 3* (*MYH3*), which have previously been shown to be expressed during myogenesis. Both *MYL2* and *MYH3*, which are marker genes [24], exhibited a gradual increase in expression rates during myogenesis, whereas *cyclin A2* (*CCNA2*), which is involved in the cell cycle [36], showed moderate and decreased expression levels (**Figure 2A**). The opposite trend was observed for *MYL2* and *MYH3*, with decreased mRNA expression, while the expression of *CCNA2* was significantly elevated as a result of $MyoG_{kd}$ (**Figure 2B**). These results are in agreement with those of our previous study [37], [38], as well as those of other investigations of mouse and human skeletal muscle differentiation [4], [39].

High-throughput sequencing

High-throughput RNA-Seq was applied to investigate the gene expression profiles of $MyoG_{wd}$ and $MyoG_{kd}$ samples. The total numbers of RNA-Seq reads (101 base pairs in length) generated in this study were about 42 million for $MyoG_{wd}$ and 46 million for

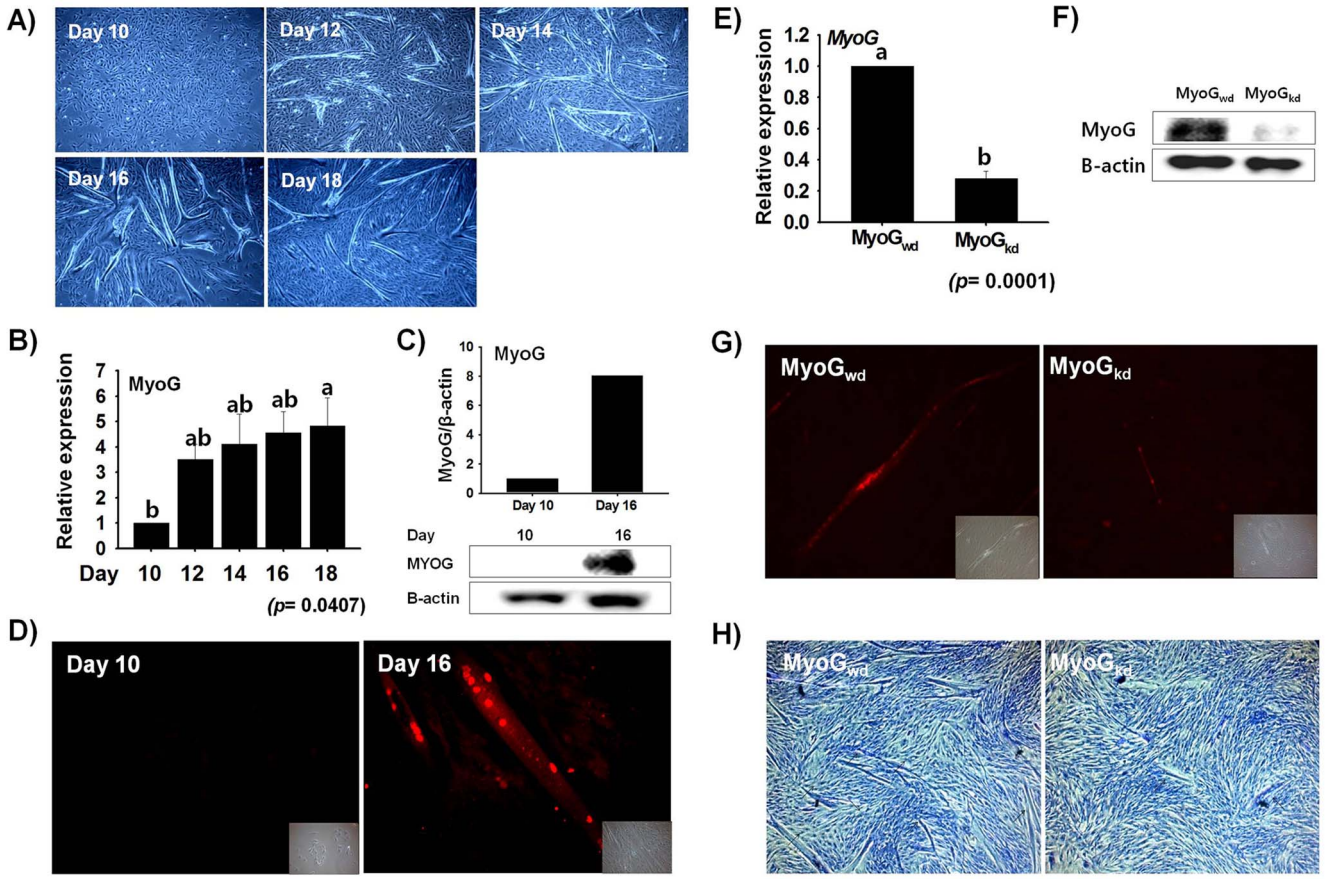

Figure 1. Myogenesis is associated with increased *MyoG* expression. A) MSCs proliferation and differentiation in DMEM/10% FBS media. Myotube formation was observed from day 12, reaching a maximum at day 16. **B**) *MyoG* expression from RNA extracted and analyzed by real time RT-PCR. *MyoG* expression gradually increased with time. **C**) MyoG protein expression at Day 10 and Day 16 was determined by Western blot analysis and the protein intensity was measured by using Image J program. MyoG protein in Day 16 cells was significantly higher than in Day 10 cells. **D**) Immunocytochemistry analysis of Day 10 and Day 16 cells stained with MyoG antibody. Day 16 showed higher MyoG nuclear expression as compared with Day 10 proliferating cells. **E)& F)** *MyoG* mRNA and protein expression of MSCs transfected with MyoG shRNA. *MyoG* expression was decreased in both RNA and protein level in $MyoG_{kd}$ cells relative to $MyoG_{wd}$ cells. **G**) Immunostaining of $MyoG_{wd}$ or $MyoG_{kd}$ cells with MyoG antibody. A significant decrease in nuclear MyoG protein expression was observed in $MyoG_{kd}$ cells. **H**) Giemsa staining performed in $MyoG_{wd}$ and $MyoG_{kd}$ cells. Myotube formation was decreased in $MyoG_{kd}$ cells relative to $MyoG_{wd}$ cells. Day 10 and $MyoG_{wd}$ represents control, respectively (mean ±S.D., n = 3). *p*-value indicates the statistical significance of the data and different letters (a and b) in graph show significant differences among groups.
doi:10.1371/journal.pone.0092447.g001

$MyoG_{kd}$. About 63.73% and 61.66% of the $MyoG_{wd}$ and $MyoG_{kd}$ reads, with at least one reported alignment, were mapped to the reference genome (**Table 1**). Post-run quality analysis of the RNA-Seq data was carried out using the FASTQC [http://www.bioinformatics.babraham.ac.uk/projects/fastqc/] tool in Galaxy [25], [26], [27]. The per base sequence quality report is one of the most useful FASTQC reports, which helps in deciding whether sequence trimming is required before alignment. **Figure 3A–D** summarizes the range of quality standards across all bases at every point in the FastQ file. For each position a boxwhisker type plot is drawn. In general, the quality of calls will degrade as the run advances, therefore, it is prevalent to see base calls falling into the orange area towards the end of a read. The quality scores across all bases were determined by the Sanger/Illumina 1.9 encoding method. These figures represent good quality calls scattered across the green background of the plots. A warning will be pointed out if the lower quartile for any base is less than 10, or if the median for any base is less than 25, whereas a failure will be issued if the lower quartile for any base is less than 5 or if the median for any base is less than 20.

Differentially expressed genes

Following mapping of the sequencing reads to the reference genome with TopHat [28], transcripts were assembled and their relative expression levels were computed with Cufflinks [31] in FPKM. A total of 13,703 unique genes were detected and further filtered to remove possible noise from the data by excluding the genes with FPKM values equal to zero from the analysis. As a result, 9,337 and 12,835 genes were identified from $MyoG_{wd}$ and $MyoG_{kd}$ samples respectively, which shared 8,469 genes in common (**Table 2**). These 8,469 genes were then used to calculate the fold change, which was defined as the ratio of $MyoG_{kd}$ FPKM to $MyoG_{wd}$ FPKM. In this study, the total fold change of ≥4 was considered to classify the differentially expressed genes. Based on this definition, there are 230 up-regulated and 224 down-regulated genes in $MyoG_{kd}$ over the $MyoG_{wd}$ sample (**Table S2**). We found that *SAP30-like* (*SAP30L*) was the most up-regulated gene in $MyoG_{kd}$ by 126-fold ($\log_2$ fold change = 6.98) and encodes a protein that plays a potential role in the histone deacetylase complex, similar to Sin3 associated protein 30 (SAP30) [40].

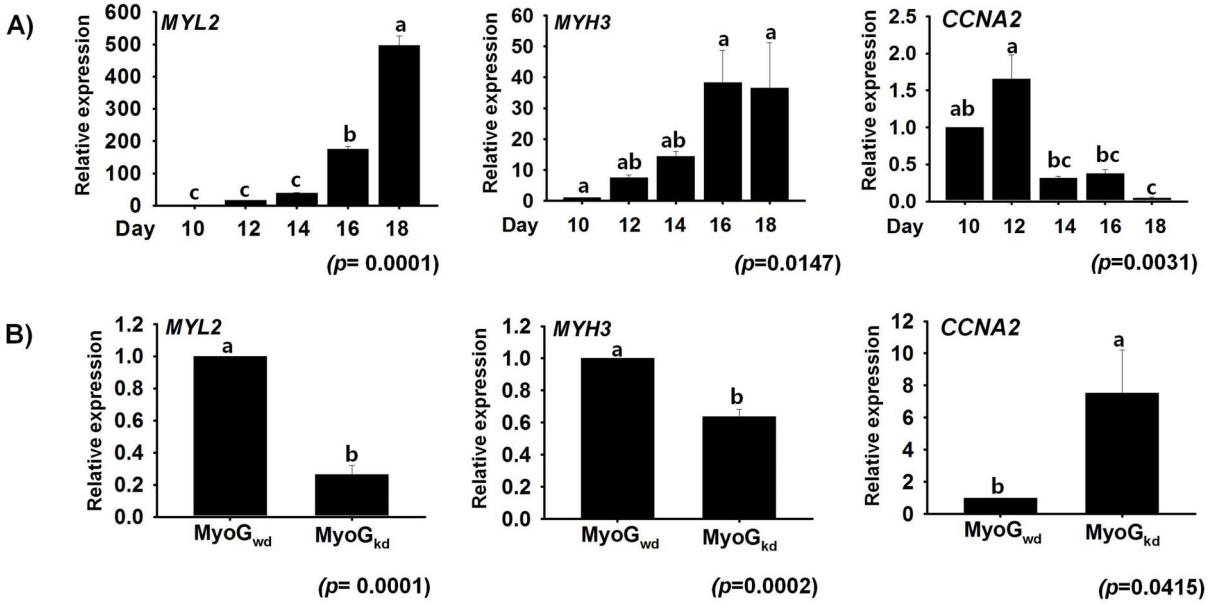

Figure 2. Effect of $MyoG_{kd}$ on *MYL2, MYH3* and *CCNA2* genes. A) Time course study of mRNA expression of *MYL2*, *MYH3* and *CCNA2* during MSCs differentiation. Cells cultured in differentiation media showed gradual increase in *MYL2* and *MYH3* expression until Day 18, but transient increase of *CCNA2* at day 12 decreased at later stage of myogenesis. **B**) Evaluation of *MYL2*, *MYH3*, and *CCNA2* gene expression by real time RT-PCR in $MyoG_{kd}$ cells. Decreased *MYL2* and *MYH3* gene expression and increased *CCNA2* expression was observed in $MyoG_{kd}$ cells relative to $MyoG_{kd}$ cells. Day 10 and $MyoG_{wd}$ represents control, respectively (mean ±S.D., n = 3). *p*-value indicates the statistical significance of the data and different letters (a, b and c) in graph show significant differences among groups.
doi:10.1371/journal.pone.0092447.g002

SAP30 was identified as one of the transcriptional regulators in C2C12 differentiation [41]. *Ribosomal protein L23a* (*RPL23A*), *zinc finger protein 322A (ZNF322A)*, *solute carrier family 16 member 3* (*SLC16A3*), *tubulin, alpha 1c* (*TUBA1C*), *sulfotransferase family, cytosolic, 2B, member 1* (*SULT2B1*), *metallothionein 2A* (*MT2A*), *matrix metallopeptidase 9* (*MMP9*), *secreted frizzled-related protein 1* (*SFRP1*) and *myelin protein* (*MBP*) were among the ten most up-regulated genes in $MyoG_{kd}$. *MT2A*, a member of cysteine-rich and metal binding intracellular proteins [42] that has been linked with cell proliferation [43], was up-regulated by 17.77-fold. In addition to *MT2A*, the other two metallothioneins (*MT1A* and *MT1E*) present in the list of differentially expressed genes also showed up-regulation by more than four-fold. Another group of highly up-regulated genes belonged to a class of matrix *metalloproteinases* (*MMPs*). A total of 13 *MMPs* were identified in this study, almost all of which showed a high fold change. *MMP1*, *MMP3*, *MMP9* (one of the ten most up-regulated genes) and *MMP13* were up-regulated by more than four-fold, whereas *MMP2* and *MMP12* were up-regulated by more than two-fold. Similarly, *MMP15*, *MMP19*, *MMP20*, *MMP23B* and *MMP27* were up-regulated by more than one-fold. Only one of the *MMPs*, *MMP16*, was down-regulated. Increased expression of *MMPs* (particularly *MMP9*) in skeletal muscles is well known [44]; therefore, our analysis is consistent with the results of previous studies. These *MMPs* enable release of the active *hepatocyte growth factor* (*HGF*), which stimulates proliferation while inhibiting differentiation, from extracellular matrix (ECM) [45]. The other genes that showed a greater than four-fold increase in expression include a transcription repressor, *musculin* also known as *MyoR* (myogenic repressor), which is known to block myogenesis and the activation of E-box dependent muscle genes [46].

Protein lyl-1 (*LYL1*), also known as *lymphoblastic leukemia-derived sequence 1*, was found to be one of the ten most down-regulated genes. *LYL1* consists of a basic helix-loop-helix (bHLH) domain (**Figure S2**), which is similar to genes involved in mammalian myogenesis (*MyoD*, *MyoG*, *Myf5*, and *herculin*) [47]. *LYL1* is an essential gene required for the development of adult hematopoietic stem cells [48]. The other ten most down-regulated genes include *sodium channel protein type 1 subunit alpha* (*SCN1A*), *ribosomal protein S15a* (*RPS15A*), *syncoilin* (*SYNC*), *tubulin alpha-1D* (*TUBA1D*), *family with sequence similarity 65, member B* (*FAM65B*), *agouti-signaling protein* (*ASIP*), *tocopherol (alpha) transfer protein-like* (*TTPAL*), *ryanodine receptor 1* (*RYR1*), and an uncharacterized protein (LOC100847946). *Myocyte enhancer factor 2C* (*MEF2C*) is a member of the *MEF2* family of transcription factors that was down-regulated by two-fold, whereas another member of the *MEF2* family, *MEF2A*, was down-regulated by about 1.5-fold. *MEF2* transcription factors play prominent roles in skeletal muscle differentiation [49], [50], and four *MEF2* isoforms (*MEF2A*, *MEF2B*, *MEF2C* and *MEF2D*) have been identified to date [51], [52]. It is well known that increased expression of *MEF2C* occurs during myoblast differentiation [53], [54], [55]. In comparison with the up-regulated genes, down-regulated genes consisted of those that play crucial roles in phosphate metabolic processes. There is a significant amount of evidence that the processes related to phosphorylation and dephosphorylation of tyrosine are important regulatory components during the progression of myogenesis [56], [57], [58], [59].

Functional annotation cluster and pathway analysis

To categorize biological processes that are overrepresented in $MyoG_{wd}$ and $MyoG_{kd}$ cells, we classified all known differentially expressed genes (fold change ≥4) using the Functional Annotation Cluster (FAC) tool available in the Database for Annotation, Visualization and Integrated Discovery (DAVID) [http://david.abcc.ncifcrf.gov/home.jsp]. DAVID FAC analysis of 230 up-regulated genes (fold change ≥4) generated a total of 65 functional clusters using default parameters. The GO terms "Biological Process", "Cellular Component" and "Molecular Function" were

Table 1. Number of single replicate RNA-Seq reads across $MyoG_{wd}$ and $MyoG_{kd}$ samples.

Sample	Total read pairs[a]	Processed reads[b]	Mapped reads[c]
$MyoG_{wd}$	42,936,654	42,910,546	27,346,293 (63.73%)
$MyoG_{kd}$	46,349,131	46,324,224	28,565,046 (61.66%)

Foot note: a. Total read count b. Reads used in TopHat process c. Reads with at least one reported alignment.
doi:10.1371/journal.pone.0092447.t001

used for annotations. Genes with a variety of GO terms from the resulting functional clusters having statistically significant *p*-values are listed in **Table 3A**. Similarly, the GO functional annotation chart reported 50 chart records that were further filtered to 22 records by selecting only those terms having *p*-values ≤0.05 and number of genes in each term ≥5 (**Table S3A**). From these tables, it can be seen that the GO terms are enriched in genes with functions necessary for actively proliferating cells such as cell division, DNA replication, cell cycle function and mitosis. The other major processes that exhibit higher levels of gene expression as a consequence of $MyoG_{kd}$ include GO terms related to organelle lumen, nucleoplasm and cytosol. These data suggest that the proliferating processes are the major processes up-regulated by $MyoG_{kd}$, and that their overrepresentation may be due to the de-differentiation of muscle cells. The down-regulation of *MyoG* in terminally differentiated mouse C2C12 myotubes was recently shown to stimulate cellular cleavage into mononucleated cells and promote cell cycle re-entry [11]. This phenomenon of dedifferentiation of myotubes into proliferating mononucleated cells is well known [60], [61], [62].

Functional analysis of 224 down-regulated genes resulted in 69 clusters, and the statistically significant (*p*-value ≤0.05) GO terms having at least five members in each enriched term are listed in **Table 3B**. The GO functional annotation chart reported 59 records, 21 of which were selected on the basis of a *p*-value ≤0.05 and number of genes in each term ≥5 (**Table S3B**). The processes that were significantly down-regulated by $MyoG_{kd}$ as shown by functional analysis include phosphate metabolic processes, dephosphorylation, phosphoprotein phosphatase activity and protein amino acid dephosphorylation. Additionally, processes related to the cell shape such as cytoskeleton and cell morphogenesis (**Table 3B & Table S3B**) were also down-

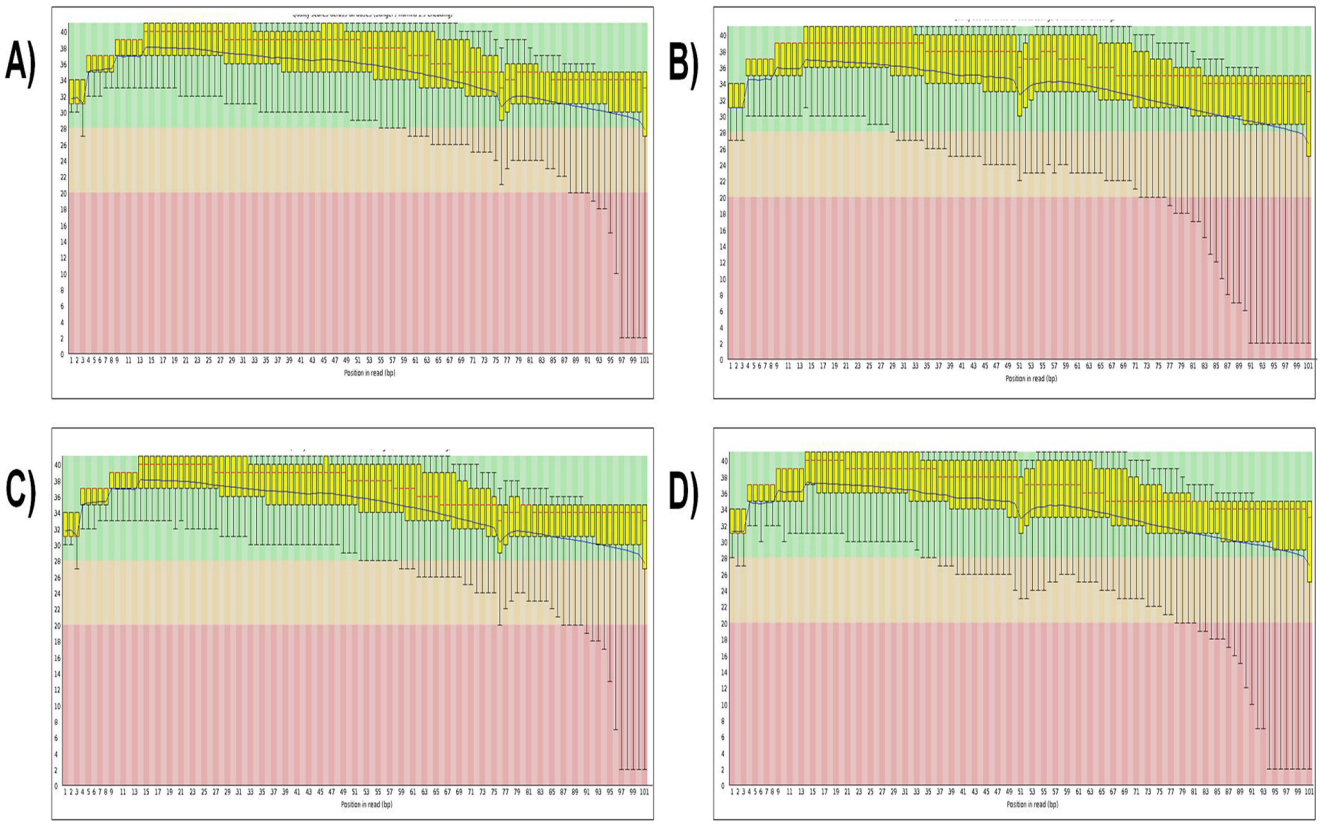

Figure 3. Per base sequence quality of $MyoG_{wd}$ and $MyoG_{kd}$. Quality scores of **A) & B)** $MyoG_{wd}$, and **C) & D)** $MyoG_{kd}$. The y-axis on the graph shows the quality scores with higher scores indicating better base calls. The background of the graph separates the y axis into high-quality calls (green), calls of reasonable quality (orange), and calls of poor quality (red). In each of these findings, the red line is the median value, the yellow box corresponds to the inter-quartile range (25–75%), the upper and lower whiskers represent the 10% and 90% points, respectively, and the blue line signifies the mean quality.
doi:10.1371/journal.pone.0092447.g003

Table 2. Gene expression summary.

Sample	$MyoG_{wd}$	$MyoG_{kd}$
Total No. of genes	9,337	12,835
Common in $MyoG_{wd}$/$MyoG_{kd}$		8,469
Up-regulated (≥4 fold)		230
Down-regulated (≥4 fold)		224

doi:10.1371/journal.pone.0092447.t002

regulated. In addition to DAVID FAC, by performing KEGG pathway analysis of 455 up- and down-regulated genes, we were able to assign 281 unique KEGG orthologs to these differentially expressed query genes. The majority of the differentially expressed genes were found to be associated with important biological processes, many being classified in signaling pathway or being involved in adhesion and cytoskeleton related functions (**Figure S3A–S3E**).

Glycogenes expression

To further explore the role of glycogenes in myogenesis, all 230 up- and 224 down-regulated genes were manually verified in the UniProt database [63] to check whether they represent a glycogene or not. If a gene encoded a protein and represented glycosyltransferases, glycosidases, lectins, sulfotransferases or proteins involved in carbohydrate metabolism or transport [5], it was labeled as a glycogene. In this way, we identified 59 (~25%) up- and 52 (~23%) down-regulated glycogenes out of 230 and 224 differentially expressed gene sets. Some of the glycogenes that demonstrated four-fold increase in expression rates included *SCNN1A*, *SFRP1* and *transmembrane protein 217* (*TMEM217*). Additionally, various glycogenes such as *matrix metalloproteinases* (*MMP1*, *MMP13*, *MMP3* and *MMP9*) and genes belonging to the solute carrier family (*SLC26A8*, *SLC2A6*, *SLC37A2* and *SLC46A3*) exhibited more than four-fold up-regulation as a consequence of $MyoG_{kd}$. Similarly, the glycogenes that showed four-fold decrease included *SCN1A*, *ASIP* and *protein wnt-11* (*WNT11*). The list of top ten up- and down-regulated genes consisted of at least two glycogenes.

Validation of RNA sequencing data

To validate the RNA-Seq results, we performed real-time RT-PCR to determine the expression levels of marker genes (*Myf5*, *MyoD*, *MyoG*, *MYL2* and *MYH3*) involved in myogenesis and then compared their expression with RNA-Seq data in $MyoG_{kd}$ samples. The RT-PCR results were well correlated with the RNA-Seq expression data for the five marker genes investigated (**Figure 4A**). Specifically, RT-PCR analysis of *Myf5*, *MyoD*, *MyoG*, *MYL2* and *MYH3* mRNA levels revealed fold changes of 0.72, 1.32, 0.42, 0.35 and 0.67, respectively (approximately >2-fold decrease) in $MyoG_{kd}$ relative to $MyoG_{wd}$ cells. These results compliment favorably well with our RNA-Seq data showing fold changes of 0.8 (*Myf5*), 2.23 (*MyoD*), 0.49 (*MyoG*), 0.33 (*MYL2*) and 0.49 (*MYH3*), which also corresponded to a two-fold decline in the expression of these marker genes. As an additional confirmation of the expression data, ten genes were randomly selected for RT-PCR analysis, five of them representing the ten most-up and down-regulated genes. The results revealed that the fold-change profiles measured by RNA-Seq and RT-PCR were concordant for all ten genes. However, RT-PCR analysis showed statistically significant expression of only eight out of these additional ten genes (**Figure 4B–K**). Among the RNA-Seq data, SAP30, *MT2A*, *sorting nexin 9* (*SNX9*), *transthyretin* (*TTR*), *and matrix gla protein* (*MGP*), were up-regulated 126.47-fold, 17.77-fold, 5.75-fold, 2.5-fold, and 2.1-fold, respectively. RT-PCR also indicated an approximately four-fold increase in expression for SAP30, MT2A whereas TTR and MGP showed about 2 fold increase in their expression. However, RT-PCR results of SNX9 exhibited about 1.4-fold increase. Similarly, *SCN1A*, *SYNC*, *RYR1*, *plexin 1* (*PLXNC1*), and *copine III* (*CPNE3*) were down-regulated by 0.01-fold, 0.02-fold, 0.08-fold, 0.13-fold, and 0.17-fold (>4-fold), respectively. However, the RT-PCR data indicated an approximately two-fold decrease in their expression levels.

Discussion

The current study offers the first thorough insight into the transcriptome analysis of primary bovine MSCs with $MYOG_{kd}$ using RNA-Seq technology. The number of total reads that map to the reference genome met the high quality criterion of the RNA-seq technology [64]. The most practical justification for reads not mapping uniquely to the reference genome could be due to the sequencing errors or polymorphisms, reads that come from repetitive sequences, and reads from exon-exon junctions [65].

Several genome wide high-throughput studies have been applied to investigate the functional role of various genes during myogenesis [4], [39], [66], [67]. Recently, a microarray based study of *MyoG* has shown its role in mediating cell cycle exit in the absence of *p38α* and recognized an important function of *p38α* in cell fusion through the up-regulation of *CD53* [68]. Another DNA microarray based study identified approximately 193 additional transcriptional regulators with varying expression levels during myogenesis [41]. DNA microarray has also been used to observe global changes in C2C12 cells transcriptome stimulated by exogenous *myostatin* (also known as *GDF8*) treatment, as well as to identify a network of genes involved in the inhibitory effects on differentiation [69]. In addition to microarray based studies, the RNA-Seq technique has been applied using C2C12 mouse myoblast cell lines to detect 13,692 known transcripts and 3,724 unannotated transcripts [29]. These sequencing or array-based methods have been shown to improve our understanding of myogenesis by revealing a broad range of target genes of myogenic transcription factors, novel myogenic factors and the characteristics of myoblasts and myotubes, which are difficult to identify by traditional approaches.

However, almost all of the aforementioned studies have used C2C12 mouse cell lines. We recently used primary bovine cells of high purity [70] to identify genes differentially expressed during differentiation and transdifferentiation of MSCs and differentiation of preadipocytes [37], [70]. MSCs are stem cells that reside between the sarcolemma and the basal lamina of adult skeletal muscle [71]. Since the serum derived from bovine species is an essential component of the *in vitro* cell culture system, there would be a great advantage of using bovine primary MSCs that closely mimic the *in vivo* situation during myogenesis [72]. Indeed, such studies might enable enhancement of muscle fiber characteristics, leading to improved meat quality. *MyoG* is specifically responsible for muscle fiber characteristics and closely associated with meat quality by affecting muscle development [73], [74].

Key processes altered during $MyoG_{kd}$

Genes involved in cell cycle regulation and DNA replication. $MyoG_{kd}$ caused up-regulation of a large number of genes involved in functions related to cell proliferation, such as DNA replication, the cell cycle and mitosis (**Table 3A & Table S3A**). **Figure 2B** verified the computational results showing that

Table 3. Significantly enriched gene ontology terms detected by FAC in A) up-regulated genes, and B) down-regulated genes.

	S. No.	GO Term (Fold enrichment)	No. of Genes	P-Value
A) Up-regulated	**1.**	GO:0005654~nucleoplasm (1.92)	22	0.0047
	2.	GO:0031981~nuclear lumen (1.54)	29	0.0189
	3.	GO:0031974~membrane-enclosed lumen (1.45)	35	0.0203
	4.	GO:0043233~organelle lumen (1.44)	35	0.0254
	5.	GO:0070013~intracellular organelle lumen (1.43)	33	0.0306
	6.	GO:0005615~extracellular space (1.91)	17	0.0157
	7.	GO:0044421~extracellular region part (1.68)	21	0.0227
	8.	GO:0004222~metalloendopeptidase activity (3.85)	5	0.0404
	9.	GO:0043933~macromolecular complex subunit organization (1.76)	16	0.037
	10.	GO:0000280~nuclear division (2.84)	8	0.0225
	11.	GO:0007067~Mitosis (2.84)	8	0.0225
	12.	GO:0000087~M phase of mitotic cell cycle (2.79)	8	0.0245
	13.	GO:0048285~organelle fission (2.73)	8	0.0272
	14.	GO:0051301~cell division (2.39)	9	0.0349
	15.	GO:0007049~cell cycle (1.71)	17	0.0384
	16.	GO:0005819~Spindle (3.14)	6	0.0418
	17.	GO:0005875~microtubule associated complex (3.77)	5	0.043
	18.	GO:0000278~mitotic cell cycle (2.11)	10	0.0469
	19.	GO:0007346~regulation of mitotic cell cycle (3.09)	6	0.0447
B) Down-regulated	**1.**	GO:0004721~phosphoprotein phosphatase activity (3.51)	7	0.0146
	2.	GO:0006470~protein amino acid dephosphorylation (3.72)	6	0.0224
	3.	GO:0016311~dephosphorylation (3.21)	6	0.0387
	4.	GO:0043292~contractile fiber (4.06)	6	0.0159
	5.	GO:0030017~sarcomere (4.18)	5	0.0312
	6.	GO:0030016~myofibril (3.69)	5	0.046
	7.	GO:0044449~contractile fiber part (3.63)	5	0.0486
	8.	GO:0000904~cell morphogenesis involved in differentiation (3.38)	10	0.0028
	9.	GO:0000902~cell morphogenesis (2.55)	11	0.0111
	10.	GO:0032989~cellular component morphogenesis (2.29)	11	0.022
	11.	GO:0031175~neuron projection development (2.58)	8	0.0355
	12.	GO:0048666~neuron development (2.19)	9	0.0529
	13.	GO:0016049~cell growth (8.11)	6	0.0008
	14.	GO:0040007~growth (3.61)	8	0.0067
	15.	GO:0008361~regulation of cell size (3.20)	8	0.0126
	16.	GO:0032535~regulation of cellular component size (2.74)	9	0.017
	17.	GO:0031090~organelle membrane (1.64)	22	0.0239
	18.	GO:0031966~mitochondrial membrane (2.08)	10	0.0506
	19.	GO:0005874~microtubule (2.69)	9	0.0186
	20.	GO:0005856~cytoskeleton (1.48)	25	0.0445
	21.	GO:0006796~ phosphate metabolic process (1.70)	20	0.0251
	22.	GO:0006793~phosphorus metabolic process (1.70)	20	0.0251
	23.	GO:0030424~axon (3.09)	6	0.0443

doi:10.1371/journal.pone.0092447.t003

CCNA2 expression increased by more than ten-fold in response to $MyoG_{kd}$ based on real time RT-PCR. Cell cycle related genes in these groups consist of several cell division homologue genes including *cell division cycle 45* (*CDC45*), *cell division cycle 20* (*CDC20*) and *cell division cycle 6* (*CDC6*), each showing more than a four-fold change. Promoter studies in quiescent myoblasts have shown that *MyoD* activates the expression of *CDC6* and *minichromosome maintenance complex component 2* (*MCM2*) genes, which prepare chromatin for DNA replication and as a result progression of the cell through the S-phase. Additionally, several other key cell division cycle-associated proteins including *cell division cycle associated 2* (*CDCA2*), *cell division cycle associated 3* (*CDCA3*), *cell division cycle associated 7* (*CDCA7*) and *cell division cycle 8* (*CDC8*) were up-regulated in response to $MyoG_{kd}$. *MyoG* plays a critical role in

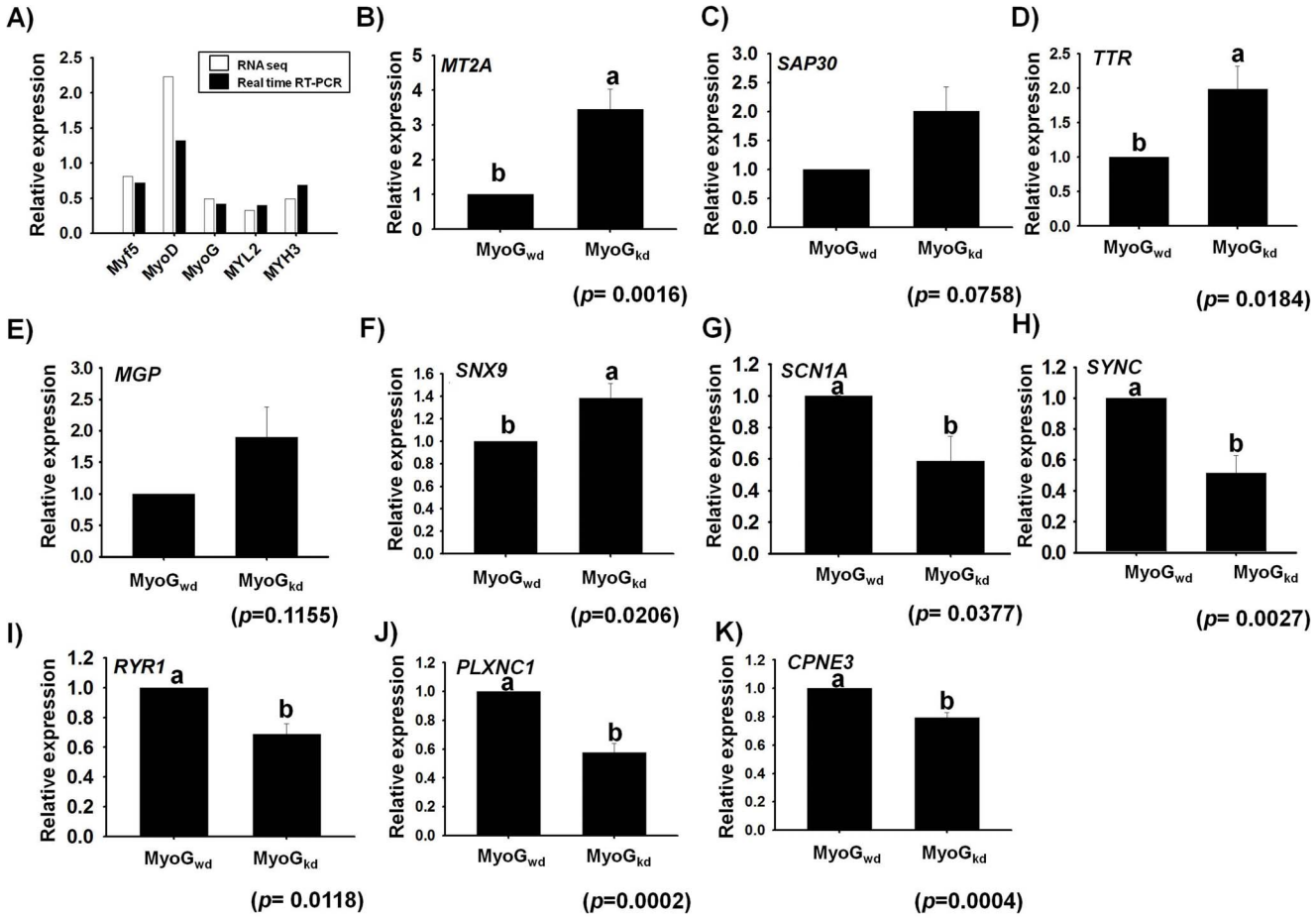

Figure 4. Real time RT-PCR validation of muscle specific and differentially expressed genes on MyoG$_{kd}$. **A**) Fold changes of *Myf5*, *MyoD*, *MyoG*, *MYL2*, and *MYH3* genes determined by RNA sequencing were compared with real-time RT PCR results. **B–K**) RT-PCR validation of mRNA expression for five randomly selected genes confirmed the increased expression of *MT2A SAP30*, *TTR*, *MGP*, and *SNX9* genes and decreased expression of *SCN1A*, *SYNC*, *RYR1*, *PLXNC1*, and *CPNE3* genes by MyoG$_{kd}$. MyoG$_{wd}$ represents control, respectively (mean ±S.D., n = 3). *p*-value indicates the statistical significance of the data and different letters (a and b) in graph show significant differences among groups.
doi:10.1371/journal.pone.0092447.g004

mediating terminal differentiation through cell cycle exit, and the activation of several cell cycle genes as a consequence of *MyoG* down-regulation is well known [68]. Among the transcription factors, *E2F transcription factor 1* (*E2F1*), which is known to play important roles in regulating cell proliferation [75], was up-regulated by about seven-fold. Previous studies have demonstrated that the expression of *MyoG* is strongly correlated with miRNA (miR-20a) expression, which in turn controls cell cycle exit by targeting E2F transcription factors [68], [76], [77], [78]. Two high mobility group box genes (*HMG20B* and *HMGA1*) that play a role in the regulation of DNA-dependent processes (transcription, replication, and DNA repair) involved in altering the conformation of chromatin also belong to this group of up-regulated biological processes [79]. Moreover, expression of MCM proteins (putative replicative helicase) such as *MCM5* is necessary for DNA replication [80], [81] and essential for DNA replication fork progression [82], [83].

Processes related to organelle lumen, nucleoplasm and cytosol. DAVID functional analysis identified 59 unique genes up-regulated by more than four-fold representing the GO terms organelle lumen, nucleoplasm and cytosol (**Table 3A and Table S3A**). These genes included transcription factor *E2F1*, *endoplasmic reticulum resident protein 44* (*ERP44*), *gamma-enolase* (*ENO2*) and *vascular endothelial growth factor-D* (*VEGF-D*), which are involved in a wide variety of biological processes. The proteins belonging to the E2F family of transcription factors play a significant role in controlling cell proliferation. For example, *E2F1* is considered the key target of pRB and is regulated by pRB throughout cell proliferation [84]. *ERP44*, a *thioredoxin* (*TRX*) family protein known to be involved in oxidative protein folding, directly regulates or inhibits the channel activity of *inositol 1,4,5-trisphosphate receptors* (*IP$_3$Rs*). *ERP44* exclusively interacts with the L3V domain of *IP$_3$R1*, and this binding is dependent on pH, Ca^{2+} concentration, and redox state [85]. *ENO2*, a membrane protein, has been reported as a marker of *neuro-muscular junctions* (*NMJs*), whose expression decreases considerably during the initial stages of human embryonic muscle tissue development [86]. *VEGF-D* interacts with, and induces dimerization and tyrosine autophosphorylation of its endothelial cell-specific receptor, *VEGFR-2*, which stimulates endothelial sprouting, proliferation, and survival, as well as vascular permeability. Similarly, binding of VEGF-D with VEGFR-3 stimulates related processes in lymphatic endothelial cells [87], [88], [89], [90].

Phosphorus metabolic process. FAC analysis identified phosphorous metabolic processes as an important biological process in MyoG$_{kd}$ cells (**Table 3B & Table S3B**). Both the FAC and function annotation chart analysis detected about 21

unique genes that exhibited ≥4-fold decrease in their expression rates and were involved in phosphorous related processes. These genes included various phosphatases and kinases such as *receptor-type tyrosine-protein phosphatase beta* (*PTPRB*), *serine/threonine-protein phosphatases PP1-beta catalytic subunit* (*PPP1CB*), *serine/threonine-protein kinase 40* (*STK40*) and *cyclin-dependent kinase 13* (*CDK13*). One of the main mechanisms by which the signaling cascades control various stages of myogenesis is through protein kinases that direct cell behavior via the reversible process of phosphorylation [91]. Extensive studies have revealed that protein tyrosine phosphatases play a vital role in regulation of skeletal muscle myogenesis [59], [92], [93], while dephosphorylation of tyrosine residues is required for cell cycle exit during myogenesis [94]. The KEGG pathway analysis identified various pathways that lead to down-regulation of various protein phosphatases during at least one step of their representative pathway, such as the PI3K-Akt signaling pathway, MAPK signaling pathway, focal adhesion, TGF-beta signaling pathway and hippo signaling pathway (**Figure 5**). One of the down-regulated genes is protein phosphatase 1, catalytic subunit, beta isozyme (*PPP1CB*), which encodes a serine/threonine-protein phosphatase PP1-beta catalytic subunit, an important enzyme responsible for protein phosphorylation and regulation of many physiological processes [95]. Pathway analysis also illustrated that *PPP1CB* is involved in many important pathways related to myogenesis such as focal adhesion, the Hippo signaling pathway and regulation of the actin cytoskeleton (**Figure S3A–E**).

Cytoskeleton and cell morphogenesis. DAVID FAC indicated that the GO terms cytoskeleton and cell morphogenesis involved in differentiation were down-regulated in response to $MyoG_{kd}$. The analyses identified about 39 unique genes involved in these processes that showed ≥4-fold reduction in their expression rates. The location of most of the genes in this category is either cytoplasm or labeled as secreted in the Uniprot database. The genes under these biological processes are involved in a broad range of functions such as signaling pathways, transport, differentiation, etc. Some of these genes include *disabled homolog 2* (*DAB2*), *microtubule-associated protein 2* (*MAP2*), *synaptopodin-2 or myopodin* (*SYNPO2*), and *moesin* (*MSN*). Among these genes, *DAB2* (expressed in various tissues), which is detected at an early myogenic differentiation state [67], has lost or reduced expression in hyperproliferative cells [96]. Another gene in this group that is significantly down-regulated is a member of the tissue inhibitors of matrix metalloproteinases (*TIMP*) family, *TIMP3*, or *metalloproteinase inhibitor 3*. *TIMP3* complexes with *MMPs* and is the only *TIMP* capable of inhibiting membrane bound *MMP*, transmembrane *MMP* and sheddases such as TNF-α converting enzyme (TACE), which is also known as disintegrin and metalloproteinase (ADAM-17) [97], [98]. Conversely, all *MMPs* detected in this study were highly up-regulated. Pathway analysis also revealed that one of the ERM proteins known to regulate cross-linking of the plasma membrane and actin cytoskeleton, *MSN*, was down-regulated [99], [100], [101].

Role of glycogene expression in myogenesis

Skeletal muscle development consists of a well controlled and regulated progression of various cellular processes, including cell proliferation, migration, and differentiation [102]. Until recently, the role of glycoproteins in myogenesis did not receive a great deal of attention from the scientific community [5], [102]. However, many independent studies have recently focused on the numerous roles of glycoconjugates during myogenesis [102]. The results of these studies have indicated that the expression of *MyoG* is partly regulated by the reduced glycosylation-dependent recruitment of *Mef2D* to *MyoG* promoter, suggesting negative regulatory mechanisms of skeletal muscle development by O-GlcNAc glycosylation [103].

Different processes related to the formation and maintenance of skeletal muscles are characterized by the expression of a wide variety of molecules that strongly alter biological events, such as muscle development, differentiation and regeneration. Among the different types of macromolecules participating in myogenesis, interest in glycoproteins has been gaining remarkable attention in recent years; however, there are still several unanswered questions regarding their roles during skeletal muscle development [102]. Similar to other eukaryotic cells, the plasma membrane and ECM of myoblasts are rich in glycoproteins and glycolipids [5]. Inhibition of some ECM proteoglycans (*syndecans*) has shown to stop the progression of myoblast proliferation and fusion, regardless of the expression of MRFs [104], [105]. Similarly, interrupting N-glycan synthesis affects myoblast fusion [106]. Glycolipids also play key roles in cell differentiation and muscle development [107], [108].

Role of channels in myogenesis

The initial phases of myogenesis are marked by the development of excitability and contractile properties by skeletal muscle cells [109]. Voltage dependent sodium channels comprise one of the key types of proteins that play a pivotal role in propagating action potential in nerves and muscle [110], [111], [112]. *SCN1A* consists of four homologous domains [113], and its activity is regulated by the interaction with *fibroblast growth factor 13* (*FGF13*) [114]. Many mutational studies have recognized a variety of tainted channel properties that include changes in the voltage dependence of activation and inactivation, speedy recuperation from inactivation, improved constant current and loss of channel function [113]. Similarly, *RYR1*, a calcium channel that plays an important role in excitation–contraction coupling in skeletal muscles, has shown increased expression levels during the early stages of myogenesis along with *dihydropyridine receptors* (*DHPRs*) [115]. *SYNC*, which belongs to the *intermediate filament* (*IF*) family of proteins [116], is greatly expressed in skeletal and cardiac muscles and may play an important role in maintaining contractile properties [117]. *SYNC* is known to interact with another member of the IF family, *desmin*, and may play a significant role in protecting muscle cells from mechanical stress [118], [119] in a fashion similar to that of other members of the IF family [120].

Together, these data offer extensive and deeper insight into the transcriptional regulation of myogenesis by *MyoG* and provide a rich scope for designing future experiments to elucidate the pathways involved in skeletal muscle differentiation. Furthermore, to improve muscle growth as well as quality and quantity of meat, it is essential to recognize how *MyoG* influences the differentiation of MSCs.

Conclusion

In summary, our transcriptome analysis of primary bovine cells using RNA-Seq offers important insight into the transcriptional regulation of gene expression in down-regulated *MyoG* muscle cells. In addition to the identification of new genes in skeletal muscle development, our bioinformatics analysis suggested a role of phosphorous metabolic processes, proteins with channeling function, and the involvement of a significant number of glycogenes in myogenesis. Further investigation of the genes identified in this study will facilitate our understanding and help explain the mechanism responsible for increasing skeletal muscle mass.

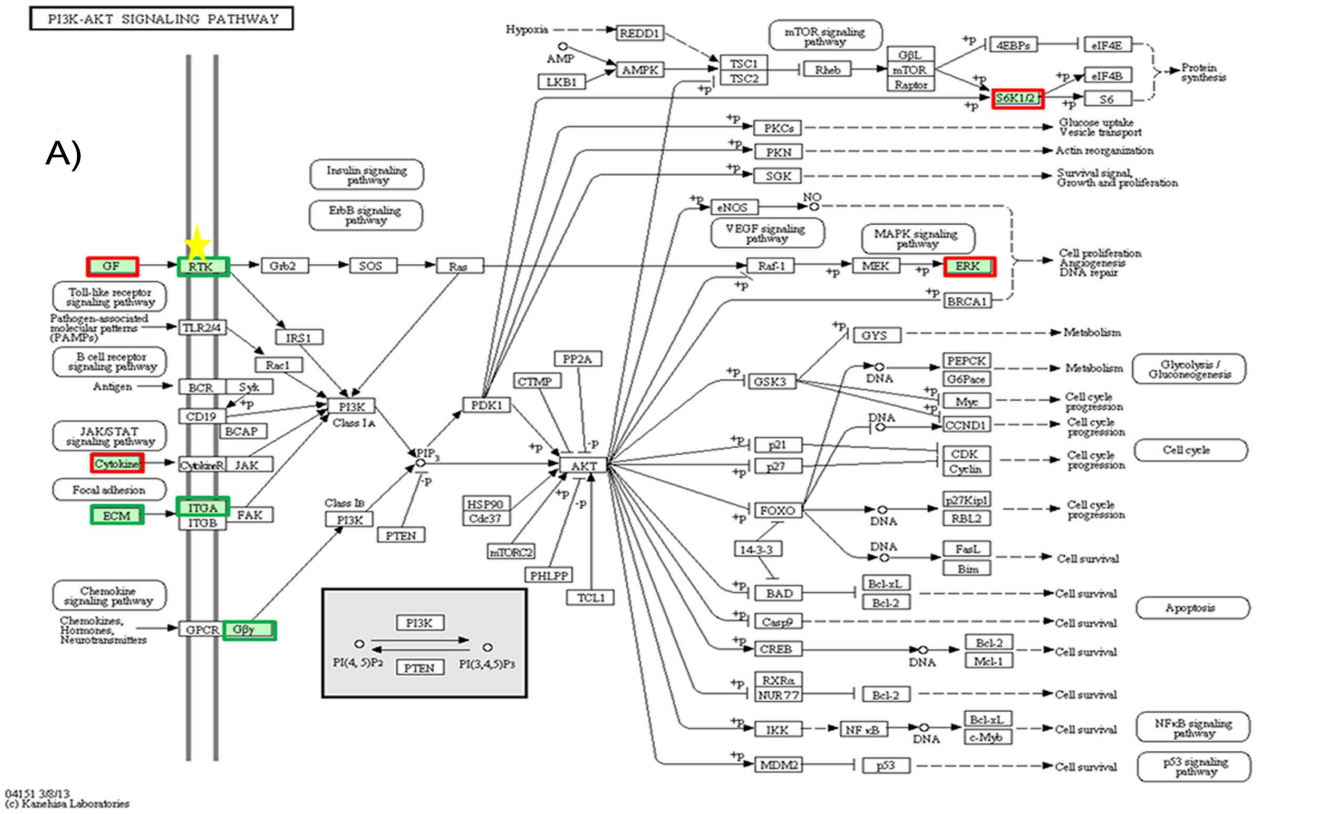
PI3K-AKT SIGNALING PATHWAY
A)
Hypoxia
AMP
REDD1
AMPK
LKB1
mTOR signaling pathway
TSC1
TSC2
Rheb
GβL
mTOR
Raptor
4EBPs
eIF4E
eIF4B
S6K1/2
S6
Protein synthesis
PKCs
PKN
SGK
Glucose uptake
Vesicle transport
Actin reorganization
Survival signal,
Growth and proliferation
Insulin signaling pathway
ErbB signaling pathway
eNOS
NO
VEGF signaling pathway
MAPK signaling pathway
GF
RTK
Grb2
SOS
Ras
Raf-1
MEK
ERK
Cell proliferation
Angiogenesis
DNA repair
BRCA1
Toll-like receptor signaling pathway
Pathogen-associated molecular patterns (PAMPs)
TLR2/4
IRS1
Rac1
B cell receptor signaling pathway
Antigen
BCR
Syk
CD19
BCAP
PI3K
Class IA
JAK/STAT signaling pathway
Cytokine
CytokineR
JAK
Focal adhesion
ECM
ITGA
ITGB
FAK
Class IB
PI3K
PTEN
PIP3
PDK1
PP2A
CTMP
HSP90
Cdc37
mTORC2
PHLPP
TCL1
AKT
GYS
Metabolism
GSK3
PEPCK
G6Pase
Metabolism
Glycolysis / Gluconeogenesis
Myc
Cell cycle progression
CCND1
Cell cycle progression
p21
p27
CDK
Cyclin
Cell cycle progression
Cell cycle
FOXO
p27Kip1
RBL2
Cell cycle progression
14-3-3
FasL
Bim
Cell survival
BAD
Bcl-xL
Bcl-2
Cell survival
Casp9
Cell survival
Apoptosis
CREB
Bcl-2
Mcl-1
Cell survival
RXRα
NUR77
Bcl-2
Cell survival
IKK
NF κB
Bcl-xL
c-Myb
Cell survival
NFκB signaling pathway
MDM2
p53
Cell survival
p53 signaling pathway
Chemokine signaling pathway
Chemokines, Hormones, Neurotransmitters
GPCR
Gβγ
PI3K
PI(4, 5)P2
PTEN
PI(3,4,5)P3
04151 3/8/13
(c) Kanehisa Laboratories

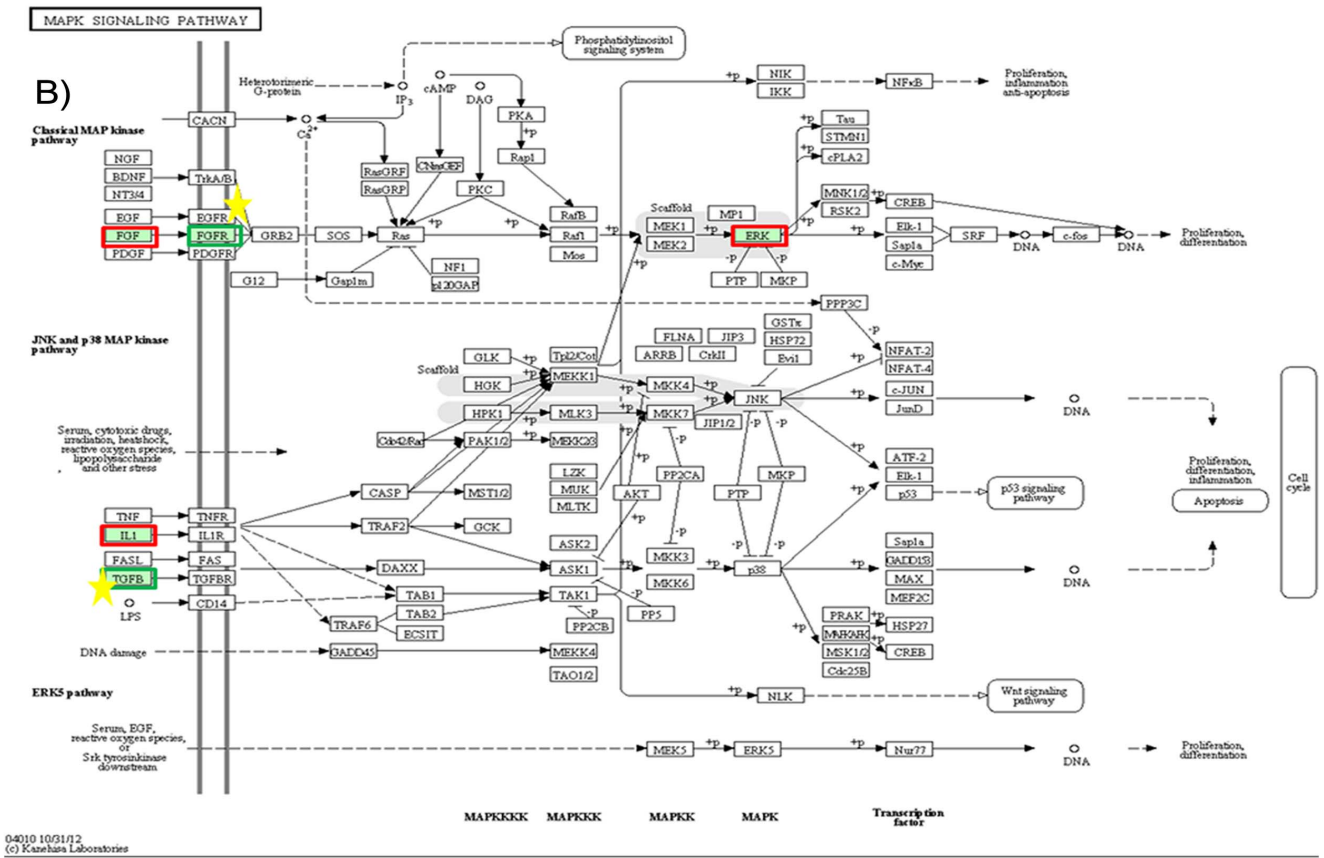
MAPK SIGNALING PATHWAY
B)
Phosphatidylinositol signaling system
Heterotrimeric G-protein
IP3
cAMP
DAG
PKA
Rap1
Classical MAP kinase pathway
CACN
Ca2+
NGF
BDNF
NT3/4
TrkA/B
EGF
EGFR
FGF
FGFR
PDGF
PDGFR
GRB2
SOS
Ras
RasGRF
CNrasGEF
RasGRP
PKC
RafB
Raf1
Mos
G12
GapIm
NF1
p120GAP
Scaffold
MEK1
MEK2
MP1
ERK
PTP
MKP
NIK
IKK
NFκB
Proliferation, inflammation anti-apoptosis
Tau
STMN1
cPLA2
MNK1/2
RSK2
CREB
Elk-1
Sap1a
c-Myc
SRF
DNA
c-fos
DNA
Proliferation, differentiation
PPP3C
JNK and p38 MAP kinase pathway
FLNA
JIP3
ARRB
CrkII
GSTκ
HSP72
Evi1
Scaffold
GLK
HGK
HPK1
Tpl2/Cot
MEKK1
MKK4
MKK7
JIP1/2
JNK
NFAT-2
NFAT-4
c-JUN
JunD
DNA
Cdc42/Rac
PAK1/2
MEKK2/3
Serum, cytotoxic drugs, irradiation, heatshock, reactive oxygen species, lipopolysaccharide and other stress
LZK
MUK
MLTK
MLK3
PP2CA
MKP
ATF-2
Elk-1
p53
p53 signaling pathway
Proliferation, differentiation, inflammation
Apoptosis
Cell cycle
CASP
MST1/2
AKT
PTP
TNF
TNFR
IL1
IL1R
TRAF2
GCK
ASK2
Sap1a
GADD45
MAX
MEF2C
FASL
FAS
TGFB
TGFBR
DAXX
ASK1
MKK3
p38
DNA
TAB1
TAK1
MKK6
LPS
CD14
TAB2
ECSIT
PP5
PP2CB
PRAK
MAPKAPK
MSK1/2
Cdc25B
HSP27
CREB
TRAF6
DNA damage
GADD45
MEKK4
TAO1/2
NLK
Wnt signaling pathway
ERK5 pathway
Serum, EGF, reactive oxygen species, or Src tyrosinkinase downstream
MEK5
ERK5
Nur77
DNA
Proliferation, differentiation
MAPKKKK
MAPKKK
MAPKK
MAPK
Transcription factor
04010 10/31/12
(c) Kanehisa Laboratories

Figure 5. KEGG pathway map analysis of differentially expressed genes (≥4-fold change). Among the various different pathways reported by KEGG analysis, two representative pathways **A**) PI3K-AKT and **B**) MAPK are shown. For each rectangular shape, red and green borders indicate up-regulated and down-regulated genes, while the yellow star indicates a role of phosphoprotein. Each KEGG pathway analysis figure depicts the role or involvement of a specific gene or a family of related genes at a particular location in the pathway. For instance, the FGF gene in KEGG MAPK pathway map represents the other FGF members (such as FGF10, FGF11, FGF12, etc) as well that may or may not be affected. Here, FGF represents all the members of fibroblast growth factor family. For FGF family members, the gene that exhibited >4 fold increase includes FGF11 whereas FGF10, FGF16, and FGF18 showed >1 fold increase in their expression rates. Conversely, the other FGF members that showed <4 fold decreased expression include FGF12 and FGF14. Similarly, FGFR represents the other members (FGFR1, FGFR2, etc) of this family of receptors as well. In case of FGFR family, FGFR2 showed >4 fold decrease in its expression, and FGFR4 exhibited >1 fold decrease in its expression rate. However, FGFR1 and FGFR3 showed about 1 fold increase in their expressions.
doi:10.1371/journal.pone.0092447.g005

Supporting Information

Figure S1 Pax7 expression in MSCs. Cellular localization of Pax7 on MSCs at Day 10 by immunocytochemistry. **A**) Cell picture **B**) DAPI-stained nuclei. **C**) Pax7 antibody stained cells.
(TIF)

Figure S2 Multiple sequence alignment of LYL1 and other bHLH genes. Multiple sequence alignment of LYL1 (UNIPROT ID: E1BAR3) protein and other bHLH proteins (MyoD, MyoG, Myf5, and herculin) which are involved in skeletal muscle development. The region in the box indicates high sequence similarity in the bHLH region of these muscle specific proteins.
(TIF)

Figure S3 Other muscle specific pathways affected by $MYOG_{kd}$. **A**) WNT signaling pathway, **B**) Focal adhesion, **C**) TGF-beta signaling pathway, **D**) Hippo signaling pathway, E) PPAR signaling pathway.
(PDF)

Table S1 Primer information.
(XLSX)

Table S2 List of up- and down-regulated genes. Each sheet contains up- and down-regulated genes separately that show at least 4 fold change in their expression.
(XLSX)

Table S3 GO functional annotation chart. GO functional annotation chart records for **A**) up-regulated genes, and **B**) Down-regulated genes. Only those terms that have p-values ≤0.05 and number of genes in each term ≥5 are shown.
(XLSX)

Acknowledgments

All research materials used in this study were provided by the Bovine Genome Resources Bank, Yeungnam University, Gyeongsan, Korea.

Author Contributions

Conceived and designed the experiments: IC EJL AM. Performed the experiments: EJL AM. Analyzed the data: EJL AM IC SP SA BAM. Contributed reagents/materials/analysis tools: KHC JK JCK DML KYC SHK. Wrote the paper: IC EJL AM SP.

References

1. Olson EN, Brennan TJ, Chakraborty T, Cheng TC, Cserjesi P, et al. (1991) Molecular control of myogenesis: antagonism between growth and differentiation. Mol Cell Biochem 104: 7–13.
2. Mohun T (1992) Muscle differentiation. Curr Opin Cell Biol 4: 923–928.
3. Andrés V, Walsh K (1996) Myogenin expression, cell cycle withdrawal, and phenotypic differentiation are temporally separable events that precede cell fusion upon myogenesis. J Cell Biol 4: 657–66.
4. Moran JL, Li Y, Hill AA, Mounts WM, Miller CP (2002) Gene expression changes during mouse skeletal myoblast differentiation revealed by transcriptional profiling. Physiol Genomics 10: 103–11.
5. Janot M, Audfray A, Loriol C, Germot A, Maftah A, et al. (2009) Glycogenome expression dynamics during mouse C2C12 myoblast differentiation suggests a sequential reorganization of membrane glycoconjugates. BMC Genomics 10: 483.
6. Rudnicki MA, Jaenisch R (1995) The MyoD family of transcription factors and skeletal myogenesis. Bioessays 17: 203–209.
7. Naya FJ, Olson E (1999) MEF2: a transcriptional target for signaling pathways controlling skeletal muscle growth and differentiation. Curr Opin Cell Biol 11: 683–688.
8. Lassar AB, Davis RL, Wright WE, Kadesch T, Murre C, et al. (1991) Functional activity of myogenic HLH proteins requires hetero-oligomerization with E12/E47-like proteins in vivo. Cell 2: 305–15.
9. Murre C, McCaw PS, Vaessin H, Caudy M, Jan LY, et al. (1989) Interactions between heterologous helix-loop-helix proteins generate complexes that bind specifically to a common DNA sequence. Cell 3: 537–44.
10. Berkes CA *and* Tapscott SJ (2005) MyoD and the transcriptional control of myogenesis. Semin Cell Dev Biol 16: 585–595.
11. Mastroyiannopoulos NP, Nicolaou P, Anayasa M, Uney JB, Phylactou LA (2012) Down-regulation of myogenin can reverse terminal muscle cell differentiation. PLOS ONE 7: e29896.
12. Kitzmann M, Carnac G, Vandromme M, Primig M, Lamb NJ, et al. (1998) The muscle regulatory factors MyoD and myf-5 undergo distinct cell cycle-specific expression in muscle cells. J Cell Biol 142: 1447–1459.
13. Molkentin JD, Olson EN (1996) Defining the regulatory networks for muscle development. Curr Opin Genet Dev 6: 445–453.
14. Rhodes SJ, Konieczny SF (1989) Identification of MRF4: a new member of the muscle regulatory factor gene family. Genes Dev 3: 2050–2061.
15. Wright WE, Sassoon DA, Lin VK (1989) Myogenin, a factor regulating myogenesis, has a domain homologous to MyoD. Cell 4: 607–17.
16. Singh K, Dilworth FJ (2013) Differential modulation of cell cycle progression distinguishes members of the myogenic regulatory factor family of transcription factors. FEBS J 280: 3991–4003.
17. Hasty P, Bradley A, Morris JH, Edmondson DG, Venuti JM, et al. (1993) Muscle deficiency and neonatal death in mice with a targeted mutation in the myogenin gene. Nature 364: 501–506.
18. Nabeshima Y, Hanaoka K, Hayasaka M, Esumi E, Li S, et al. (1993) Myogenin gene disruption results in perinatal lethality because of severe muscle defect. Nature 364: 532–535.
19. Rawls A, Morris JH, Rudnicki M, Braun T, Arnold HH, et al. (1995) Myogenin's functions do not overlap with those of MyoD or Myf-5 during mouse embryogenesis. Dev Biol 172: 37–50.
20. Myer A, Olson EN, Klein WH (2001) MyoD cannot compensate for the absence of myogenin during skeletal muscle differentiation in murine embryonic stem cells. Dev Biol 229: 340–350.
21. Rudnicki MA, Braun T, Hinuma S, Jaenisch R (1992) Inactivation of MyoD in mice leads to up-regulation of the myogenic HLH gene Myf-5 and results in apparently normal muscle development. Cell 3: 383–90.
22. Zhang W, Behringer RR, Olson EN (1995) Inactivation of the myogenic bHLH gene MRF4 results in up-regulation of myogenin and rib anomalies. Genes Dev 11: 1388–1399.
23. Meadows E, Cho JH, Flynn JM, Klein WH (2008) Myogenin regulates a distinct genetic program in adult muscle stem cells. Dev Biol 322: 406–414.
24. Lee EJ, Prati Bajracharya, Lee DM, Kang SW, Lee YS, et al. (2012) Gene expression profiles during differentiation and transdifferentiation of bovine myogenic satellite cells. Genes & Genomics 34: 133–148.
25. Giardine B, Riemer C, Hardison RC, Burhans R, Elnitski L, et al. (2005) Galaxy: a platform for interactive large-scale genome analysis. Genome Res 15: 1451–1455.
26. Blankenberg D, Gordon A, Von Kuster G, Coraor N, Taylor J, et al. (2010) Manipulation of FASTQ data with Galaxy. Bioinformatics 26: 1783–1785.
27. Goecks J, Nekrutenko A, Taylor J, Afgan E, Ananda G, et al. (2010) Galaxy: a comprehensive approach for supporting accessible, reproducible, and transparent computational research in the life sciences. Genome Biol 11: R86.

28. Trapnell C, Pachter L, Salzberg SL (2009) TopHat: discovering splice junctions with RNA-Seq. Bioinformatics 25: 1105–1111.
29. Langmead B, Trapnell C, Pop M, Salzberg SL (2010) Ultrafast and memory-efficient alignment of short DNA sequences to the human genome. Genome Biol 10: R25.
30. Altschul SF, Gish W, Miller W, Myers EW, Lipman DJ (1990) Basic local alignment search tool. J Mol Biol 215: 403–10.
31. Trapnell C, Williams BA, Pertea G, Mortazavi A, Kwan G, et al. (2010) Transcript assembly and quantification by RNA-Seq reveals unannotated transcripts and isoform switching during cell differentiation. Nat Biotechnol 28: 511–515.
32. Moriya Y, Itoh M, Okuda S, Yoshizawa AC, Kanehisa M (2007) KAAS: an automatic genome annotation and pathway reconstruction server. Nucleic Acids Res 35: W182–185.
33. Wright WE, Sassoon DA, Lin VK (1989) Myogenin, a factor regulating myogenesis, has a domain homologous to MyoD. Cell 4: 607–17.
34. Delgado I, Huang X, Jones S, Zhang L, Hatcher R, et al. (2003) Dynamic gene expression during the onset of myoblast differentiation in vitro. Genomics 2: 109–21.
35. Janot M, Audfray A, Loriol C, Germot A, Maftah A, et al. (2009) Glycogenome expression dynamics during mouse C2C12 myoblast differentiation suggests a sequential reorganization of membrane glycoconjugates. BMC Genomics 10: 483.
36. Henglein B, Chenivesse X, Wang J, Eick D, Bréchot C (1994) Structure and cell cycle-regulated transcription of the human cyclin A gene. Proc Natl Acad Sci U S A 91: 5490–4.
37. Lee EJ, Lee HJ, Kamli MR, Pokharel S, Bhat AR, et al. (2012) Depot-specific gene expression profiles during differentiation and transdifferentiation of bovine muscle satellite cells, and differentiation of preadipocytes. Genomics 100: 195–202.
38. Lee EJ, Bhat AR, Kamli MR, Pokharel S, Chun T, et al. (2013) *Transthyretin* Is a Key Regulator of Myoblast Differentiation. PLOS ONE 8: e63627.
39. Sterrenburg E, Turk R, 't Hoen PA, van Deutekom JC, Boer JM, et al. (2004) Large-scale gene expression analysis of human skeletal myoblast differentiation. Neuromuscul Disord 14: 507–518.
40. Lindfors K, Viiri KM, Niittynen M, Heinonen TY, Mäki M, et al. (2003) TGF-beta induces the expression of SAP30L, a novel nuclear protein. BMC Genomics 1: 53.
41. Rajan S, Chu Pham Dang H, Djambazian H, Zuzan H, et al. (2012) Analysis of early C2C12 myogenesis identifies stably and differentially expressed transcriptional regulators whose knock-down inhibits myoblast differentiation. Physiol Genomics 2: 183–197.
42. Jin R, Chow VT, Tan PH, Dheen ST, Duan W, et al. (2002) Metallothionein 2A expression is associated with cell proliferation in breast cancer. Carcinogenesis 23: 81–86.
43. Cherian MG, Apostolova MD (2000) Nuclear localization of metallothionein during cell proliferation and differentiation. Cell Mol Biol 46: 347–356.
44. Dahiya S, Bhatnagar S, Hindi SM, Jiang C, Paul PK, et al. (2011) Elevated levels of active matrix metalloproteinase-9 cause hypertrophy in skeletal muscle of normal and dystrophin-deficient mdx mice. Hum Mol Genet 20: 4345–4359.
45. Bentzinger CF, von Maltzahn J, Rudnicki MA (2010) Extrinsic regulation of satellite cell specification. Stem Cell Res Ther 1: 27.
46. Lu J, Webb R, Richardson JA, Olson EN (1999) MyoR: a muscle-restricted basic helix-loop-helix transcription factor that antagonizes the actions of MyoD. Proc Natl Acad Sci USA 2: 552–557.
47. Miyamoto A, Cui X, Naumovski L, Cleary ML (1996) Helix-loop-helix proteins LYL1 and E2a form heterodimeric complexes with distinctive DNA-binding properties in hematolymphoid cells. Mol Cell Biol 16: 2394–2401.
48. Souroullas GP, Salmon JM, Sablitzky F, Curtis DJ, Goodell MA (2009) Adult hematopoietic stem and progenitor cells require either Lyl1 or Scl for survival. Cell Stem Cell 4: 180–186.
49. Molkentin JD, Black BL, Martin JF, Olson EN (1995) Cooperative activation of muscle gene expression by MEF2 and myogenic bHLH proteins. Cell 83: 1125–1136.
50. Brand-Saberi B, Christ B (1999) Genetic and epigenetic control of muscle development in vertebrates. Cell Tissue Res 296: 199–212.
51. Brand NJ (1997) Myocyte enhancer factor 2 (MEF2). Int J Biochem Cell Biol 12: 1467–1470.
52. Black BL, Olson EN (1998) Transcriptional control of muscle development by myocyte enhancer factor-2 (MEF2) proteins. Annu Rev Cell Dev Biol 14: 167–196.
53. McDermott JC, Cardoso MC, Yu YT, Andres V, Leifer D, et al. (1993) hMEF2C gene encodes skeletal muscle- and brain-specific transcription factors. Mol Cell Biol 13: 2564–2577.
54. Martin JF, Miano JM, Hustad CM, Copeland NG, Jenkins NA, et al. (1994) A Mef2 gene that generates a muscle-specific isoform via alternative mRNA splicing. Mol Cell Biol 14: 1647–1656.
55. Al-Khalili L, Krämer D, Wretenberg P, Krook A. (2004) Human skeletal muscle cell differentiation is associated with changes in myogenic markers and enhanced insulin-mediated MAPK and PKB phosphorylation. Acta Physiol Scand. 180: 395–403.
56. Lin X, Yang X, Li Q, Ma Y, Cui S, et al. (2012) Protein tyrosine phosphatase-like A regulates myoblast proliferation and differentiation through MyoG and the cell cycling signaling pathway. Mol Cell Biol 32: 297–308.
57. Quach NL, Rando TA (2006) Focal adhesion kinase is essential for costamerogenesis in cultured skeletal muscle cells. Dev Biol 293: 38–52.
58. Kaliman P, Viñals F, Testar X, Palacín M, Zorzano A (1996) Phosphatidylinositol 3-kinase inhibitors block differentiation of skeletal muscle cells. J Biol Chem 271: 19146–19151.
59. Fornaro M, Burch PM, Yang W, Zhang L, Hamilton CE, et al. (2006) SHP-2 activates signaling of the nuclear factor of activated T cells to promote skeletal muscle growth. J Cell Biol 175: 87–97.
60. McGann CJ, Odelberg SJ, Keating MT (2001) Mammalian myotube dedifferentiation induced by newt regeneration extract. Proc Natl Acad Sci USA 98: 13699–13704.
61. Odelberg SJ, Kollhoff A, Keating MT (2000) Dedifferentiation of mammalian myotubes induced by msx1. Cell 103: 1099–1109.
62. Jung DW, Williams DR (2011) Novel Chemically Defined Approach To Produce Multipotent Cells from Terminally Differentiated Tissue Syncytia. ACS Chem Biol 6: 553–562.
63. Bairoch A, Apweiler R, Wu CH, Barker WC, Boeckmann B, et al. (2005) The Universal Protein Resource (UniProt). Nucleic Acids Res 33: D154–9.
64. Mortazavi A, Williams BA, McCue K, Schaeffer L, Wold B (2008) Mapping and quantifying mammalian transcriptomes by RNA-Seq. Nat Methods 5: 621–8.
65. Marioni JC, Mason CE, Mane SM, Stephens M, Gilad Y (2008) RNA-seq: an assessment of technical reproducibility and comparison with gene expression arrays. Genome Res 18: 1509–17.
66. Shen X, Collier JM, Hlaing M, Zhang L, Delshad EH, et al. (2003) Genome-wide examination of myoblast cell cycle withdrawal during differentiation. Dev Dyn 1: 128–138.
67. Tomczak KK, Marinescu VD, Ramoni MF, Sanoudou D, Montanaro F, et al. (2004) Expression profiling and identification of novel genes involved in myogenic differentiation. FASEB J 18: 403–405.
68. Liu QC, Zha XH, Faralli H, Yin H, Louis-Jeune C, et al. (2012) Comparative expression profiling identifies differential roles for Myogenin and p38α MAPK signaling in myogenesis. J Mol Cell Biol 4: 386–397.
69. Wicik Z, Sadkowski T, Jank M, Motyl T (2011) The transcriptomic signature of myostatin inhibitory influence on the differentiation of mouse C2C12 myoblasts. Pol J Vet Sci 4: 643–652.
70. Lee EJ, Kamli MR, Pokharel S, Malik A, Tareq KMA, et al. (2013) Expressed Sequence Tags for Bovine Muscle Satellite Cells, Myotube Formed-Cells and Adipocyte-Like Cells. PLOS ONE doi 10.1371/journal.pone.0079780.
71. Asakura A, Komaki M, Rudnicki M (2001) Muscle satellite cells are multipotential stem cells that exhibit myogenic, osteogenic, and adipogenic differentiation. Differentiation 68: 245–253.
72. Lee DM, Bajracharya P, Lee EJ, Kim JE, Lee HJ et al. (2011) Effects of gender-specific adult bovine serum on myogenic satellite cell proliferation, differentiation and lipid accumulation. In Vitro Cell Dev Biol-Anim 47: 438–444.
73. Wang Q, Liu YP, Jiang XS, Yang CW, DU HR, et al. (2008) Correlation analysis of relationships between polymorphisms of high quality chicken myogenin gene and slaughter and meat quality traits. Front Agric China 2: 512–518.
74. Kim JM, Choi BD, Kim BC, Park SS, Hong KC (2009) Associations of the variation in the porcine myogenin gene with muscle fibre characteristics, lean meat production and meat quality traits. J Anim Breed Genet 126: 134–141.
75. Wang C, Rauscher FJ 3rd, Cress WD, Chen J (2007) Regulation of E2F1 function by the nuclear corepressor KAP1. J Biol Chem 282: 29902–29909.
76. O'Donnell KA, Wentzel EA, Zeller KI, Dang CV, Mendell JT (2005) c-Myc-regulated microRNAs modulate E2F1 expression. Nature 435: 839–843.
77. Sylvestre Y, De Guire V, Querido E, Mukhopadhyay UK, Bourdeau V, et al. (2007) An E2F/miR-20a autoregulatory feedback loop. J Biol Chem 282: 2135–2143.
78. Nagel S, Venturini L, Przybylski GK, Grabarczyk P, Schmidt CA, et al. (2009) Activation of miR-17-92 by NK-like homeodomain proteins suppresses apoptosis via reduction of E2F1 in T-cell acute lymphoblastic leukemia. Leuk Lymphoma 50: 101–108.
79. Thomas JO (2001) HMG1 and 2: architectural DNA-binding proteins. Biochem Soc Trans 29: 395–401.
80. Tye BK (1999) MCM proteins in DNA replication. Annu Rev Biochem 68: 649–686.
81. Forsburg SL (2004) Eukaryotic MCM proteins: beyond replication initiation. Microbiol Mol Biol Rev 68: 109–131.
82. Labib K, Kearsey SE, Diffley JF (2001) MCM2-7 proteins are essential components of prereplicative complexes that accumulate cooperatively in the nucleus during G1-phase and are required to establish, but not maintain, the S-phase checkpoint. Mol Biol Cell 12: 3658–3667.
83. Pacek M, Walter JC (2004) A requirement for MCM7 and Cdc45 in chromosome unwinding during eukaryotic DNA replication. EMBO J 23: 3667–3676.
84. Sahin F, Sladek TL (2010) E2F-1 has dual roles depending on the cell cycle. Int J Biol Sci 2: 116–128.
85. Higo T, Hattori M, Nakamura T, Natsume T, Michikawa T, et al. (2005) Subtype-specific and ER lumenal environment-dependent regulation of inositol 1,4,5-trisphosphate receptor type 1 by ERp44. Cell 1: 85–98.

86. Merkulova T, Dehaupas M, Nevers MC, Créminon C, Alameddine H, et al. (2000) Differential modulation of α, β and γ enolase isoforms in regenerating mouse skeletal muscle. European Journal of Biochemistry 267: 3735–3743.
87. Achen MG, Jeltsch M, Kukk E, et al. (1998) Vascular endothelial growth factor D (VEGF-D) is a ligand for the tyrosine kinases VEGF receptor 2 (Flk1) and VEGF receptor 3 (Flt4). Proc Natl Acad Sci USA 2: 548–553.
88. Shibuya M, Claesson-Welsh L (2006) Signal transduction by VEGF receptors in regulation of angiogenesis and lymphangiogenesis. Exp Cell Res 5: 549–560.
89. Tammela T, Alitalo K (2010) Lymphangiogenesis: molecular mechanisms and future promise. Cell 4: 460–476.
90. Leppänen VM, Jeltsch M, Anisimov A, Tvorogov D, Aho K, et al. (2011) Structural determinants of vascular endothelial growth factor-D receptor binding and specificity. Blood 117: 1507–1515.
91. Knight JD, Kothary R (2011) The myogenic kinome: protein kinases critical to mammalian skeletal myogenesis. Skelet Muscle 1: 29.
92. Hinard V, Belin D, Konig S, Bader CR, Bernheim L (2008) Initiation of human myoblast differentiation via dephosphorylation of Kir2.1 K+ channels at tyrosine 242. Development 135: 859–867.
93. Lu H, Shah P, Ennis D, Shinder G, Sap J, et al. (2002) The differentiation of skeletal muscle cells involves a protein-tyrosine phosphatase-alpha-mediated C-Src signaling pathway. J Biol Chem 277: 46687–46695.
94. De Oliveira MV, Marin TM, Clemente CF, Costa AP, Judice CC, et al. (2009) SHP-2 regulates myogenesis by coupling to FAK signaling pathway. FEBS Lett 583: 2975–2981.
95. Huang T, Xiong YZ, Lei MG, Xu DQ, Deng CY (2006) Identification of a differentially expressed gene PPP1CB between porcine Longissimus dorsi of Meishan and Large WhitexMeishan hybrids. Acta Biochim Biophys Sin 38: 450–456.
96. Fazili Z, Sun W, Mittelstaedt S, Cohen C, Xu XX (1999) Disabled-2 inactivation is an early step in ovarian tumorigenicity. Oncogene 18: 3104–13.
97. Amour A, Slocombe PM, Webster A, Butler M, Knight CG, et al. (1998) TNF-alpha converting enzyme (TACE) is inhibited by TIMP-3. FEBS Lett 435: 39–44.
98. Shen Y, Winkler IG, Barbier V, Sims NA, Hendy J, et al. (2010) Tissue inhibitor of metalloproteinase-3 (TIMP-3) regulates hematopoiesis and bone formation in vivo. PLOS ONE 5: e13086.
99. Fehon RG, McClatchey AI, Bretscher A (2010) Organizing the cell cortex: the role of ERM proteins. Nat Rev Mol Cell Biol 11: 276–87.
100. Tsukita S, Yonemura S (1999) Cortical actin organization: lessons from ERM (ezrin/radixin/moesin) proteins. J Biol Chem 274: 34507–10.
101. Henning MS, Stiedl P, Barry DS, McMahon R, Morham SG, et al. (2011) PDZD8 is a novel moesin-interacting cytoskeletal regulatory protein that suppresses infection by herpes simplex virus type 1. Virology 415: 114–21.
102. Brandan E, Gutierrez J (2013) Role of skeletal muscle proteoglycans during myogenesis. Matrix Biol 32: 289–297.
103. Ogawa M, Sakakibara Y, Kamemura K (2013) Requirement of decreased O-GlcNAc glycosylation of Mef2D for its recruitment to the myogenin promoter. Biochem Biophys Res Commun. 433: 558–62.
104. Osses N, Brandan E (2002) ECM is required for skeletal muscle differentiation independently of muscle regulatory factor expression. Am J Physiol Cell Physiol 282: C383–394.
105. Cornelison DD, Wilcox-Adelman SA, Goetinck PF, Rauvala H, Rapraeger AC, et al. (2004) Essential and separable roles for Syndecan-3 and Syndecan-4 in skeletal muscle development and regeneration. Genes Dev 18: 2231–2236.
106. Metzler M, Gertz A, Sarkar M, Schachter H, Schrader JW, et al. (1994) Complex asparagine-linked oligosaccharides are required for morphogenic events during post-implantation development. EMBO J 13: 2056–2065.
107. Fukumoto S, Iwamoto T, Sakai E, Yuasa K, Fukumoto E, et al. (2006) Current topics in pharmacological research on bone metabolism: osteoclast differentiation regulated by glycosphingolipids. J Pharmacol Sci 100: 195–200.
108. Yanagisawa M, Yu RK (2007) The expression and functions of glycoconjugates in neural stem cells. Glycobiology 17: 57R–74R.
109. Ugarte G, Brandan E (2006) Transforming growth factor beta (TGF-beta) signaling is regulated by electrical activity in skeletal muscle cells. TGF-beta type I receptor is transcriptionally regulated by myotube excitability. J Biol Chem 27: 18473–18481.
110. Yu FH, Catterall WA (2003) Overview of the voltage-gated sodium channel family. Genome Biol 4: 207.
111. Hodgkin AL, Huxley AF, Katz B (1952) Measurement of current-voltage relations in the membrane of the giant axon of Loligo. J Physiol 116: 424–448.
112. Martínez-Mármol R, David M, Sanches R, Roura-Ferrer M, Villalonga N, et al. (2007) Voltage-dependent Na+ channel phenotype changes in myoblasts. Consequences for cardiac repair. Cardiovasc Res 3: 430–41.
113. Barela AJ, Waddy SP, Lickfett JG, Hunter J, Anido A, et al (2006) An epilepsy mutation in the sodium channel SCN1A that decreases channel excitability. J Neurosci 10: 2714–23.
114. Wang C, Wang C, Hoch EG, Pitt GS (2011) Identification of novel interaction sites that determine specificity between fibroblast growth factor homologous factors and voltage-gated sodium channels. J Biol Chem 27: 24253–63.
115. Vega AV, Ramos-Mondragón R, Calderón-Rivera A, Zarain-Herzberg A, Avila G (2011) Calcitonin gene-related peptide restores disrupted excitation-contraction coupling in myotubes expressing central core disease mutations in RyR1. J Physiol 19: 4649–4669.
116. Newey SE, Howman EV, Ponting CP, Benson MA, Nawrotzki R, et al. (2001) Syncoilin, a novel member of the intermediate filament superfamily that interacts with alpha-dystrobrevin in skeletal muscle. J Biol Chem 9: 6645–6655.
117. McCullagh KJ, Edwards B, Kemp MW, Giles LC, Burgess M, et al. (2008) Analysis of skeletal muscle function in the C57BL6/SV129 syncoilin knockout mouse. Mamm Genome 5: 339–351.
118. Capetanaki Y, Bloch RJ, Kouloumenta A, Mavroidis M, Psarras S (2007) Muscle intermediate filaments and their links to membranes and membranous organelles. Exp Cell Res 10: 2063–2076.
119. Costa ML, Escaleira R, Cataldo A, Oliveira F, Mermelstein CS (2004) Desmin: molecular interactions and putative functions of the muscle intermediate filament protein. Braz J Med Biol Res 12: 1819–1830.
120. Parry DA, Strelkov SV, Burkhard P, Aebi U, Herrmann H (2007) Towards a molecular description of intermediate filament structure and assembly. Exp Cell Res 10: 2204–2216.